EasyChair Preprint

№ 5869

Numerical Simulation of Impacted Elastic Bar

Adib Hamdani and Pankaj Pankaj

June 23, 2021

https://doi.org/10.31436/iiumej.vxxixx.xxxx

NUMERICAL SIMULATION OF IMPACTED ELASTIC BAR

ADIB HAMDANI[1,2*], PANKAJ PANKAJ[2]

[1]*Department of Mechanical Engineering, International Islamic University Malaysia, Malaysia*
[2]*Institute for Bioengineering, The University of Edinburgh, Edinburgh, United Kingdom*

**Corresponding author: hadib@iium.edu.my*

(Received: Day Month Year; Accepted: Day Month Year; Published on-line: Day Month Year)

ABSTRACT: This numerical analysis considers a model of an elastic cylindrical bar impacted by rigid mass, which its accuracy is benchmarked by a closed-form solution developed for this impact process. The analytical solution provides theoretical background and understanding, however, practical problem is not always restricted to a simple one-dimensional geometry and boundary conditions of a purely elastic material behaviour. Hence, the current work numerically simulates the impacted elastic bar, then explores parameters which are not considered in its theoretical model. A two-dimensional (2D) solid axisymmetric system is considered, in which rigid impactor is assigned with initial velocity corresponding to certain drop height and a 2D contact type is defined between interacting bodies. Both elastic and time-dependent viscoelastic material models are considered in this study. The simulation results reveal time intervals gradually increase in every sequential intervals, while relatively small discrepancies are recorded for peak load and pulse width outputs. The parameters of impactor's mass, drop height and structural stiffness are varied; showing how these parameters individually affect the resulting force response at end struck. The models then evaluate time-dependent viscoelastic material model; showing stiffer response of the resulting force in comparison to models assigned with long-term elastic moduli. Derived elastic modulus-output variable relations show comparable mathematical forms to corresponding equations formulated analytically.

KEY WORDS: *Numerical method, Force at end struck, Parameter-output variable relations and Viscoelasticity.*

1. INTRODUCTION

This numerical work simulates an impact problem based on [1], which involves a restrained elastic bar subjected to rigid mass as shown in Fig. 1. The simulation is undertaken using a finite element (FE) commercial package, LS-DYNA (smp d R7.1.1, LSTC, Livermore, California). The available analytical model is considered as the bar is treated as purely elastic, then it is extended to more complex time-dependent elastic behaviour. The study also evaluates relations between several parameters and corresponding output variables.

2. PROBLEM DEFINITION

Consider a stationary elastic cylinder with diameter, $2r$, and length, l, subjected to impact due to an incoming rigid impactor at one end (called the end struck), while the other end is restrained as shown in Fig. 1. Numerical solutions are important as not all problems are elastic, have a simple one-dimensional geometry and boundary conditions as in theoretical model by [1,2]; consequently, closed-form solutions are not possible. The closed-form solutions, however, help in evaluating and benchmarking the accuracy of numerical methods, such as this attempted work.

https://doi.org/10.31436/iiumej.vxxixx.xxxx

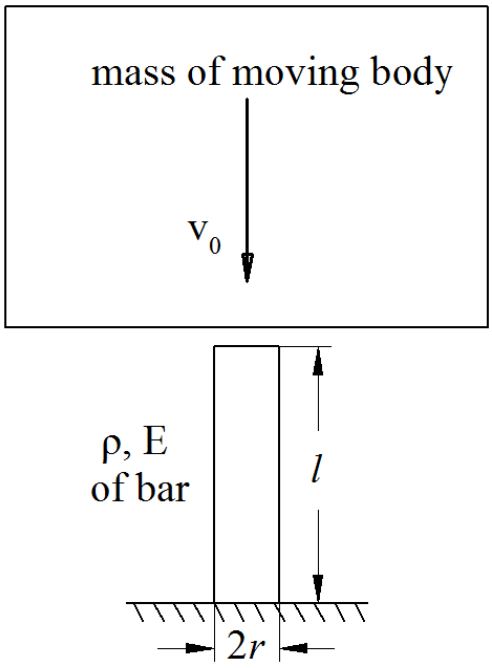

Fig. 1. Axial impact problem [1] to be numerically modelled.

Explicit code of LS-DYNA is utilised for this work, which uses explicit time integration based on central difference method (CDM) to obtain nodal displacements from their velocities and accelerations in every time step. The time step is calculated by the programme at every stage in simulation by dividing the smallest characteristic length with the continuum wave speed [3]; indicating the time required for wave speed to traverse the smallest element.

3. NUMERICAL MODEL

FE analysis requires four basic main inputs: the geometry with corresponding FE mesh; boundary conditions defined for the models; load application and the material behaviour of the models. This section discusses the definitions for each of these required inputs in the current study.

3.1. Discretisation of axisymmetric system

Impact mechanics involves more than one body in the collision [4], which implies the necessity of defining a minimum of two geometrical models. Planar symmetryof the cylindrical shape in the defined problem as shown in Fig. 2 is exploited. Two-dimensional (2D) solid models in LS-DYNA are based on integral difference scheme, which defines the geometries in global XY plane. In axisymmetric case, radial direction corresponds to X-axis, while the axis of symmetry lies on the Y-axis. LS-DYNA offers two options of axisymmetric elements, namely Petrov-Galerkin and Galerkin finite element approaches, generally referred as ‘area-weighted’ and ‘volume-weighted’ methods respectively. The former is designed suitably for situations where the developed pressures in the model constitute a large fraction of the elastic modulus, i.e. a hydrodynamic case [3].

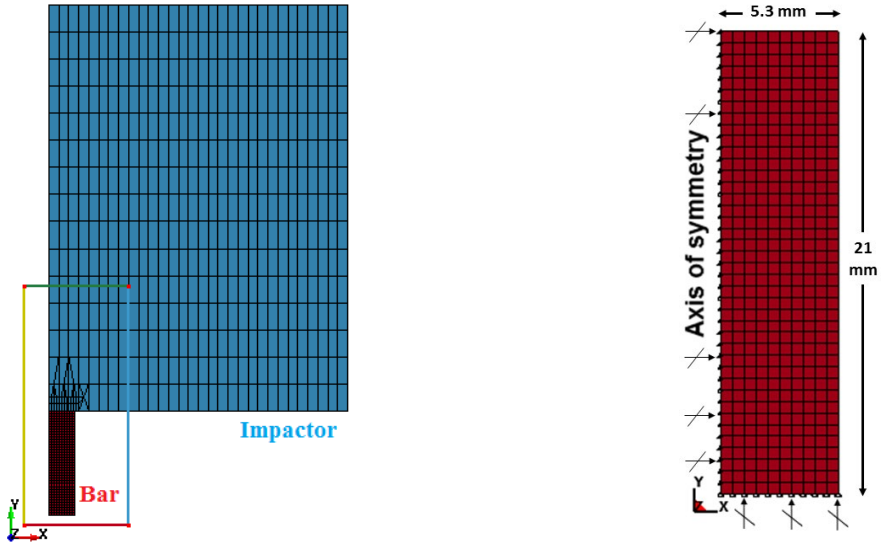

(a) Axisymmetric element (b) Dimensions and constraints

Fig. 2. Finite element (FE) models. The box in (a) focuses on the region of interest.

The volume-weighted Galerkin method is chosen in this work since there is no possibility of a hydrodynamic scenario arising in the problems being considered. The bar is discretised into 4-noded axisymmetric 10×40 elements to provide almost square 2D elements, with similar 1:2 diameter-to-length ratio (Fig. 2b). The rest of this primitive geometry are theoretically revolved 2π radians around the axis of symmetry to create a virtual cylindrical model of the bar as shown in Fig. 2.

Accordingly, the impactor is also assumed to have axisymmetric shape with arbitrary radius-length dimension, while ensuring the impactor's mass is 2.5 kg simulating the experimental drop test or around 26.6 g for a light-weight dropped hammer following [3]. Figure 2(a) shows the impactor as coarsely meshed in order to reduce the computational cost, while refinement is applied at the bottom elements which involve with contacting the end struck of the bar. This mesh refinement is required to ensure each slave node (on the impactor) are properly projected to its master segment (the bar struck). Node-collapsing method is applied to some three-noded elements in this region of refined mesh.

3.2 Boundary conditions

By the definition of axisymmetry in LS-DYNA, the global Y-axis represents theaxis of symmetry, which for the problem considered automatically constrains the nodes on this axis in the global X-translation (radial). In addition, all bottom nodes are restrained in vertical direction as shown in Fig. 2(b) which is sufficient and consistent with the closed-form model in Fig. 1.

3.3 Loading conditions: Contact and initial velocity

Contact definition is required to establish interaction between the contacting surfaces of impactor and bar. The contact definition allows the incoming slave nodes of the impactor to recognise the top of the bar (which contains master segments). The mesh refinement size between the two contacting models is comparable. Standard penalty-based contact is employed for this purpose, which uses numerical springs to prevent penetration of each slave nodes through master segments as well as to transfer loads between contacting parts [3].

The *2D Automatic Surface to Surface* contact type is employed which uses penalty forces to prevent penetration between external faces of 2D continuum elements. In addition, *Force Transducer* option is used in conjunction with the previous contact card to measure forces

generated by that contact definition. In the current axisymmetric model, the force output is per unit radian. Normal direction of both slave and master surfaces are determined automatically by the programme, in which the initial model set up already has orthogonal contact surfaces prior to the impact [3].

The hammer is assigned with corresponding initial velocity from drop height with only small gap is introduced between the models in order to avoid initial penetration leading to instability in the calculation of the contact forces [3]. The gap size is generally balanced between minimising initial computational cost (caused by a large gap) and avoiding initial penetration (due to gap being too small) between contacting solids. The best decision depends on the pre-calculation of the defined time step of the smallest element, the initial distance between the first expected contacting elements and the assigned nodal velocity.

3.4 Material models

The bar's material is defined as elastic, which is similar to the closed-form solution in [1,2], or viscoelastic. The impactor is defined as rigid material which matches the problem definition and justifies the irregular mesh of the impactor near the impacted region. In addition, this material model is a cost effective option because its model does not store history variables due to its undeformed body restriction.

Even though the rigid definition itself implies infinite stiffness, values of both Young's modulus, and Poisson's ratio need to be assigned to determine the bulk modulus for calculating the contact stiffness. In addition, the explicit time integration requires the mass density of the impactor in order to construct mass matrix in the CDM solution for the nodal displacements, even though the wave propagation is not calculated for the rigid material.

4. COMPARISON WITH THE CLOSED-FORM SOLUTION

The force response of a cylindrical FE model (10.6 mm diameter and 12 mm length) impacted by a light-weight 26.6-g hammer is first compared with the closed-form (CF) solution in terms of the resulting peak load and pulse width. The solid axisymmetric bar is converted to a one-dimensional model by assuming the Poisson's ratio to be zero, i.e. there is no transverse response in the 2D solid element. The light hammer is chosen to increase the mass ratio, which in turn would result in only seven stress intervals in the pulse response, allowing easy comparison to be made.

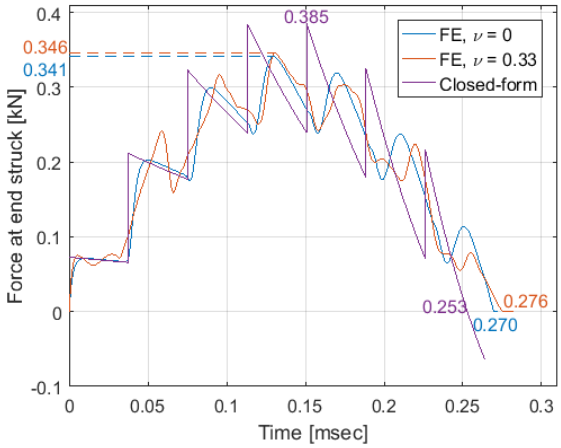

Fig. 3. Verifying force response from FE of zero Poisson's ratio ($\nu = 0$) with the closed-form solution [2]. The effect of a non-zero ν FE model is also shown.

Fig. 3 compares the FE response (zero Poisson's ratio) to that from the closed-form solution. It can be seen that there are seven force intervals in both FE and closed-form responses, which they are similar in the form of bell-like shape. The sharp peak-and-trough of vertical shape in every interval due to the instantaneous rise of force by CF solution [1,2] is not recreated by the numerical simulation, nonetheless it is still fairly visible.

It is apparent that the closed-form solution returns consistent time interval, following strictly the governing equation of interval time [1,2], whereas this time from FE solution gradually increases in every sequential interval. This discrepancy is explainable by understanding the ideal scenario in the closed-form solution in which the supposed deformation of bar is neglected in the analysis. Onthe other hand, the FE model experiences numerical damping which is a default setting for all contact options in the LS-DYNA [3] causing longer time for the travelling stress wave. Table 1 shows comparison of the two main outputs under investigation, namely peak load ($F_{\max}$) and pulse width (t_{pulse}) between the two solutions. The FE method records 11.43% lower peak load, while its pulse width is 6.72% larger in comparison to its benchmark results by the CF solution.

Table 1: Comparing one-dimensional FE model ($\nu = 0$) with the closed-form solution

Output variables	**Peak load [kN]**			**Pulse width [msec]**		
Models	**FE**	**CF**	**% diff.**	**FE**	**CF**	**% diff.**
	0.341	0.385	-11.43	0.27	0.253	6.72

The effect of Poisson's ratio ($\nu = 0.33$) is shown in Fig. 3, in which higher frequency distortion in its overall resulting pulse pattern is observed causing slightly unclear pattern of seven intervals. This happens perhaps due to the effect of wave bouncing from the sides. Nonetheless, the following peak load and pulse width values are not significantly affected, such that only 1.5% and 2.2% differences with the one-dimensional FE model. It can be concluded that assigning a reasonable value of Poisson's ratio does not drastically alter the response, in particular the output variables under interest, which are $F_{\max}$ and t_{pulse}.

5. EFFECT OF DIFFERENT PARAMETERS ON THE RESULTING ELASTIC PULSE

The effect of varying several parameters: mass of impactor;drop height; and structural stiffness; towards the resulting force at end struck by using numerical simulation is considered. This elastic study of axial impact on trabecular bone samples is based on report by [2]; some of the parameters are not varied, i.e. density: $\rho = 1.31 \times 10^{-6}\ \text{kg/mm}^3$; bar's length, $l = 21$ mm; and Poisson's ratio, $\nu = 0.33$. The axisymmetric model is discretised using 10×40 elements in radial and axial directions respectively, which is almost 1:1 of bar's diameter-to-length ratio or even slightly less for models with smaller radius. The analysed output is the summation of eleven (11) nodal forces histories of the nodes at the top of axisymmetric bar model, multiplied by 2π to obtain the total force acting on the surface of end struck.

5.1 Impactor's mass and drop height

Two values of impactor's mass are chosen, which are 1.807 and 2.5 kg, while the two drop heights are 100 and 200 mm, making up four (4) FE models for this analysis. The models have geometry of 10.6 mm of diameter and 21 mm of length, with elastic modulus is assigned to be 531 MPa as reported by [5] and falls within ranges reported by many studies including [6-11] for trabecular bone. The drop height affects only the peak load, while pulse width is independent of this input parameter as shown in Fig. 4; this finding by numerical method is consistent with theoretical parametric analysis in [2]; it was also shown in the study the peak

https://doi.org/10.31436/iiumej.vxxixx.xxxx

load has direct proportionality to the square-root of drop height, h. As can be seen from Fig. 4 , this is satisfied by the numerical solution. The pulse width is also almost identical for impactors of the same mass dropped from different heights. Fig. 4 also shows that a higher drop height results in a fractionally smaller pulse width.

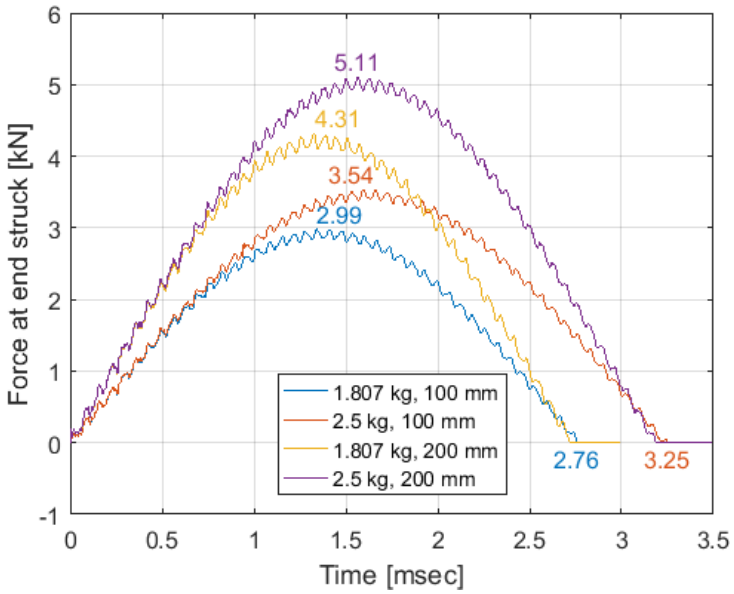

Fig. 4. Effect of drop height, h and impactor's mass, m_{impactor} on the resulting force at end struck.

A larger mass of the impactor leads to larger peak loads and also pulse width, which is consistent to the analysis of the closed-form solution in [2]. In addition, it is observed in Fig. 4 that with the increase in m_{impactor}, the force responses appear to be almost similar initially, then the load for higher mass increases at a substantially higher rate and as expected comprises of larger number of stress intervals.

5.2 Structural stiffness

The structural stiffness of a simple column under compressive load is a function of its material (Young's modulus) and dimensions (cross-sectional area and length). The pulse exhibits stiffer response when the combination of higher peak load and lower pulse width is obtained [2].

In this parametric study, 2.5 kg impactor is dropped from 100 mm height. The parametric study with respect to length was examined in the closed-form solution [2], therefore only elastic modulus and diameter (representing area) are varied in this analysis. Similar elastic modulus of 531 MPa is chosen,with addition of arbitrary materially-stiffer models of 1 GPa. The diameters are either 10.6 mm [2] or 8.6 mm, in which a smaller area is expected to exhibit a less stiff behaviour.

https://doi.org/10.31436/iiumej.vxxixx.xxxx

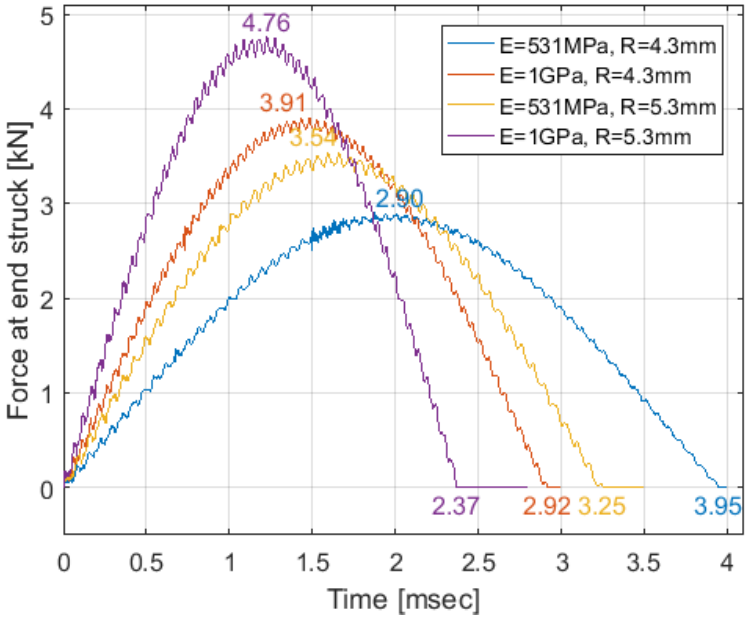

Fig. 5. Effect of structural stiffness (elastic modulus, *E* and radius, *R* representing material and geometry components respectively) on the resulting force at end struck.

The resulting force responses at the end struck are shown in Fig. 5 for four varying-stiffness models. The stiffest response is shown by the model with highest elastic modulus and cross-sectional area, i.e E = 1 GPa, radius, R = 5.3 mm; followed by models with lower structural stiffness contributors. These demonstrate the influence of elastic modulus and cross-sectional diameter on the peak load and the pulse width. The peak load is seen to be directly proportional to the elastic modulus as would be expected [2]. The peak load is also directly proportional to the cross-sectional area. The effect on pulse width is simply the opposite to that for the peak load, i.e. pulse width decreases with increase in elastic modulus and radius.

6. IMPACT RESPONSE OF MODELS WITH TIME-DEPENDENT MATERIAL BEHAVIOUR

The effect of employing a time-dependent material model, viz. viscoelasticity (VE) is analysed in comparison to simple time-independent linear elastic model (abbreviated as TI-E) assigned to the impacted axisymmetric bar. In VE material model, the relaxation modulus can be defined using the Prony series [12] as

$$E(t) = E_{\text{eqm}} + \sum_{i=1}^{n} E_i e^{-\frac{t}{\rho_i}}, \quad (1)$$

where E_{eqm} is the equilibrium modulus and E_i and ρ_i are the relaxation strengths and relaxation times respectively. A three-term Prony series ($n = 3$) was shown to adequately represent the relaxation modulus of trabecular bone with different volume fractions, BV/TV [13]. The values determined in this above cited study are used to consider the influence of time-dependent material properties on impact response.

6.1 Implementing viscoelasticity in LS-DYNA

In TI-E model, single value of elastic modulus, E is taken as $E(\infty)$ or E_{eqm} from Eq. 1; a long- term modulus representing the material resistance value when the load stabilises hence treated as in statically-applied manner in equilibrium. On the other hand, the viscoelastic

https://doi.org/10.31436/iiumej.vxxixx.xxxx

material model in LS-DYNA, e.g. Mat076: General Viscoelastic requires elastic bulk modulus, K. Similar to the equilibrium modulus in TI-E, K in VE is defined as a long-term modulus. The Poisson's ratio was defined as 0.33. In order to exhibit relaxation phase in the VE model, shear relaxation moduli, $G_i$and decay constants, β_i for each term in Prony series are required. Hence, the general expression of the Prony series in LS-DYNA is

$$g(t) = \sum_{i=1}^{n} G_i e^{-\beta_i t}. \qquad (2)$$

Comparing these two relaxation expressions in Eqs. (1-2), the relaxation strengths and times parameters in Eq. (1) provided by [13] need to be converted onto shear moduli and decay constants in Eq. (2) respectively. Shear moduli are obtained from E and ν assuming isotropic behaviour while the decay constants (βi) are simply inverse of the relaxation times (ρi) in which $i = 1, 2, 3$ for three terms of Prony series. In the case of three-term Prony series, the General Viscoelastic material model requires four input terms, in which the extra term is G_{eqm} with zero decay constant, fully expressed as

$$g(t) = G_{\text{eqm}} + G_1 e^{-\beta_1 t} + G_2 e^{-\beta_2 t} + G_3 e^{-\beta_3 t}. \qquad (3)$$

Six (6) bone volume fraction models, i.e. BV/TV=19, 26, 33, 39, 42 and 43% are selectively chosen from [13] on the basis of signifying direct correlation between material's stiffness and the reported BV/TV. The required input parameters are given in Table 2 by using moduli conversions into Eq. 3. All these conversions are applicable in this study assuming the material as having isotropic behaviour.

Table 2: Parameters of time-independent elastic (TI-E) and viscoelastic (VE) material models; Units: modulus [MPa], decay constant [ksec^{-1}]

BV/TV [%]	TI-E	VE adopting Prony series				
	E_{eqm}	K_{eqm}	G_{eqm}	i	G_i	β_i
0.19	250.43	417.38	89.44	1	5.34	684.93
				2	3.27	42.39
				3	5.90	3.75
0.26	317.18	528.63	113.28	1	7.80	1111.11
				2	5.55	119.76
				3	6.61	8.22
0.33	498.53	830.88	178.05	1	12.18	1086.96
				2	6.51	125.47
				3	6.83	10.24
0.39	545.65	909.42	194.88	1	15.17	1351.35
				2	10.55	129.03
				3	11.99	6.76
0.42	572.05	953.42	204.30	1	16.32	3030.30
				2	10.74	184.84
				3	10.66	9.10
0.43	904.68	1507.80	323.10	1	24.34	1010.10
				2	12.40	109.53
				3	19.95	7.15

6.2 Force response

The bar is discretised into 4-noded axisymmetric 10 × 40 solid elements impacted by a 2.5-kg rigid impactor. The length, l of the bar is 21 mm and its diameter, $2r$ is 10.6 mm. The impactor was assigned with axial velocity of 0.99 m/s, which is equivalent when it is dropped from 50 mm height. In order to terminate the simulation, the pulse duration is estimated [1,2] as

$$t_{\text{pulse}} \approx \frac{1}{r}\sqrt{\frac{m_{\text{impactor}}\pi l}{E}}, \qquad (4)$$

then the termination time was set to be slightly longer than the estimated pulse width in Eq. 4.

Two main outputs are investigated from the resulting force response at the end struck of axisymmetric bar, namely the peak load as the highest magnitude of compressive load experienced by the end struck and the pulse width, which is the contact duration of the impact incidence. Fig. 6 shows graphical elastic and viscoelastic responses of three different BV/TVs, clearly depicts that viscoelastic models have stiffer response than their TI-E counterparts.

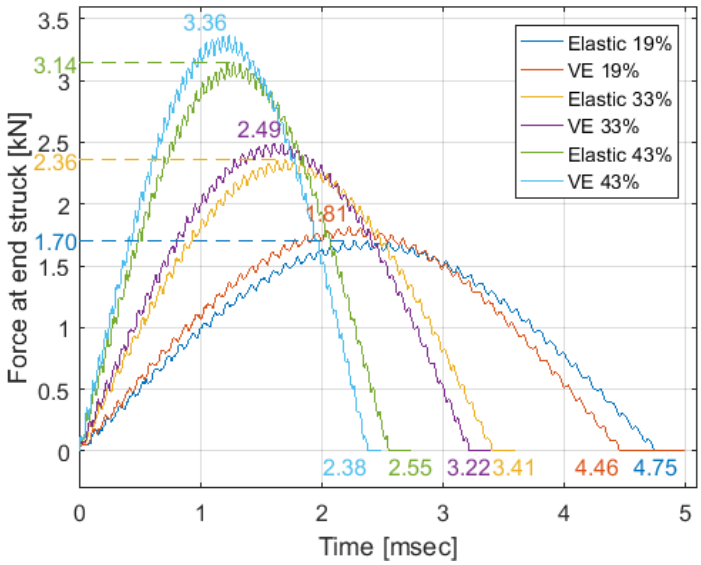

Fig. 6. Effect of varying time-independent and viscoelastic properties towards peak load and pulse width.

The key numerical results for all models are tabulated in Table 3 with $E(t)$ represents E_{eqm} and $E(0)$ for TI-E and VE respectively. The modulus function $E(t)$ represents well the contribution of BV/TV to bone sample's stiffness for both material models. In addition, the stiffness of VE models, which is $E(0)$ is consistently higher than TI-E (E_{eqm}).

Table 3: Elastic modulus input of time-independent elastic (TI-E) and viscoelastic (VE) material properties with the corresponding peak load (F_{max}) and pulse width (t_{pulse})

BV/TV	Model	E(t) [MPa]	Peak load [kN]		Pulse width [msec]	
			Value [kN]	% diff.	Value [kN]	% diff.
19%	TI-E	250.4	1.7037	6.53	4.7549	6.14
	VE	291.1	1.8150		4.4629	
26%	TI-E	317.2	1.9036	7.31	4.2455	6.75
	VE	373.1	2.0428		3.9591	

https://doi.org/10.31436/iiumej.vxxixx.xxxx

33%	**TI-E**	498.5	2.3580	5.55	3.4111	5.57
	VE	570.0	2.4889		3.2212	
39%	**TI-E**	545.7	2.4641	7.39	3.2646	7.16
	VE	651.2	2.6461		3.0310	
42%	**TI-E**	572.1	2.5223	7.34	3.1919	6.71
	VE	677.7	2.7074		2.9777	
43%	**TI-E**	904.7	3.1434	6.94	2.5544	6.67
	VE	1063.4	3.3615		2.3839	

Based on peak load values in Table 3, the corresponding maximum compressive stresses at end struck fall in the range of $19.3 \leq \sigma_{\max} \leq 38.1$ MPa as simulated by FE method. As comparison, trabecular bone was reported to have yield strength of 17.45 ± 6.15 MPa and $5 - 20$ MPa by [14] and [15], who used extensometer and split Hopkinson pressure bar respectively. Maximum compressive stresses from Table 3 recorded higher values than these reported strengths, nonetheless they were proven experimentally to be realistic in drop tests [2].

6.3 Modulus-to-output variable relations

The parametric study in [2] points to the requirement of using linear direct best fit regression for relating $\sqrt{E}$ to the peak load i.e. $F_{\max} \propto \sqrt{E}$. On the other hand, its effect on the pulse width is inversely proportional or negative power law i.e. $t_{\text{pulse}} \propto 1/\sqrt{E}$. The mathematical relations obtained from this numerical analysis is shown in Fig. 7.

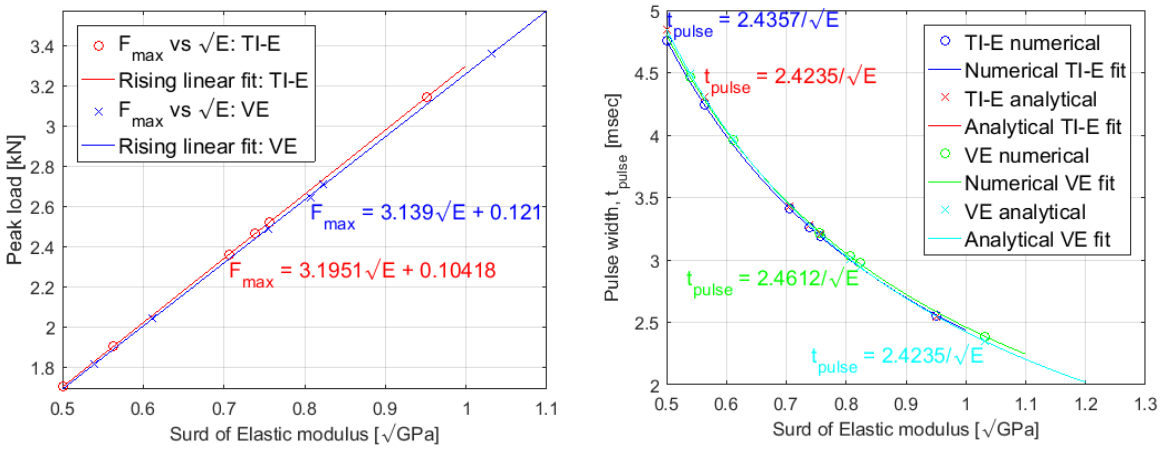

(a) $F_{\max} - \sqrt{E}$ direct proportionality (b) $t_{\text{pulse}} - \sqrt{E}$ inverse proportionality

Fig. 7. Output variables relations with elastic modulus for varying material properties.

The output variable-elastic modulus relations in Fig. 7 show very close resemblance to the mathematical relations derived from the closed-form solution provided by [2] i.e. similar regression models return almost identical constants. Hence, it can be concluded that the current FE models well replicate the theoretical solutions, hence they are benchmarked and could be used for more complex axial bar impact problems.

7. SUMMARY

This numerical work replicates an axial bar subjected to rigid mass impactor problem as described in [1,2]. Sufficiently-refined volume-weighted Galerkin axisymmetric elements model is used which is available in LS-DYNA as a cost-effective geometrical model, while linear elastic and time-dependent viscoelastic material models were evaluated. The study is successfully validated by theoretical solutions by [2] in which comparable results were obtained when analysing: 1) the effect of Poisson's ratio; 2) parametric study on impactor's mass, drop height and structural stiffness; and 3) output variable relations (peak load and pulse width) with square-root of elastic modulus. Hence, the FE models developed in this study are successfully benchmarked and can be further developed for incorporating more complex inputs from axial bar impact problems.

ACKNOWLEDGEMENT

The first author is indebted to the Ministry of Education, Malaysia for the award of PhD sponsorship.

REFERENCES

[1] Timoshenko S, Goodier JN. (1951) Theory of Elasticity, 2nd Ed. McGraw-Hill Book Company, Inc., New York.
[2] Rosli AHB. (2019) Characterisation of Trabecular Bone Behaviour under Impact, PhD Thesis, The University of Edinburgh.
[3] LSTC. (2017) LS-DYNA® Theory Manual, Technical Report, Livermore Software Technology Corporation (LSTC), Livermore, California.
[4] Stronge WJ. (2000) Impact Mechanics, Cambridge University Press.
[5] Xie S, Wallace RJ, Callanan A, Pankaj P. (2018) From Tension to Compression: Asymmetric Mechanical Behaviour of Trabecular Bone's Organic Phase. Annals of Biomedical Engineering, 46(6):801-809.
[6] Lotz JC, Gerhart TN, Hayes WC. (1990) Mechanical Properties of Trabecular Bone from the Proximal Femur: A Quantitative CT Study. Journal of Computer Assisted Tomography, 14(1):107-114.
[7] Keller TS. (1994) Predicting the Compressive Mechanical Behaviour of Bone. Journal of Biomechanics, 27(9):1159-1168.
[8] Goulet RW, Goldstein SA, Ciarelli MJ, Kuhn JL, Brown MB, Feldkamp LA. (1994) The Relationship between the Structural and Orthogonal Compressive Properties of Trabecular Bone. Journal of Biomechanics, 27(4):375-389.
[9] Li B, Aspden RM. (1997) Composition and Mechanical Properties of Cancellous Bone from the Femoral Head of Patients with Osteoporosis or Osteoarthritis. Journal of Bone Mineral Research, 12(4):450-456.
[10] Ciarelli TE, Fyhrie DP, Schaffler MB, Goldstein SA. (2000) Variations in Three-dimensional Cancellous Bone Architecture of the Proximal Femur in Female Hip Fractures and in Controls. Journal of Bone and Mineral Research, 15(1):32-40.
[11] Kaneko TS, Bell JS, Pejcic MR, Tehranzadeh J, Keyak JH. (2004) Mechanical Properties, Density and Quantitative CT Scan Data of Trabecular Bone with and without Metastases. Journal of Biomechanics, 37(4):523-530.
[12] Park SW, Schapery RA. (1999) Methods of Interconversion between Linear Viscoelastic Material Functions. Part I-a Numerical Method Based on Prony Series. International Journal of Solids and Structures, 36(11):1653-1675.
[13] Manda K, Xie S, Wallace RJ, Levrero-Florencio F, Pankaj P. (2016) Linear Viscoelasticity – Bone Volume Fraction Relationships of Bovine Trabecular Bone. Biomechanics and Modeling in Mechanobiology, 15(6):1631-1640.

[14] Morgan EF, Keaveny TM. (2001) Dependence of Yield Strain of Human Trabecular Bone on Anatomic Site. Journal of Biomechanics, 34:569-577.
[15] Shim V, Yang L, Liu J, Lee V. (2005) Characterisation of the Dynamic Compressive Mechanical Properties of Cancellous Bone from the Human Cervical Spine. International Journal of Impact Engineering, 32(1-4):525-540.